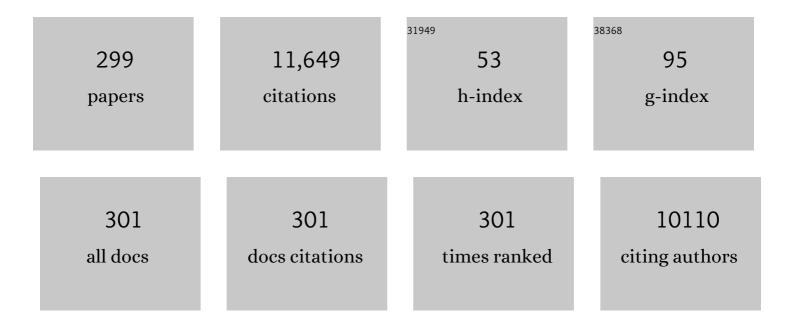
List of Publications by Year in descending order

Source: https://exaly.com/author-pdf/6528349/publications.pdf

Version: 2024-02-01



#	Article	IF	CITATIONS
1	Exchange bias in nanostructures. Physics Reports, 2005, 422, 65-117.	10.3	1,722
2	Experimental parameters influencing grain refinement and microstructural evolution during high-pressure torsion. Acta Materialia, 2003, 51, 753-765.	3.8	717
3	Synthesis and Size-Dependent Exchange Bias in Inverted Coreâ^'Shell MnO Mn3O4Nanoparticles. Journal of the American Chemical Society, 2007, 129, 9102-9108.	6.6	261
4	Cubic versus Spherical Magnetic Nanoparticles: The Role of Surface Anisotropy. Journal of the American Chemical Society, 2008, 130, 13234-13239.	6.6	226
5	Orientation imaging microscopy of ultrafine-grained nickel. Scripta Materialia, 2002, 46, 575-580.	2.6	217
6	The microstructural characteristics of ultrafine-grained nickel. Materials Science & Engineering A: Structural Materials: Properties, Microstructure and Processing, 2005, 391, 377-389.	2.6	185
7	Robust antiferromagnetic coupling in hard-soft bi-magnetic core/shell nanoparticles. Nature Communications, 2013, 4, 2960.	5.8	160
8	Mg–Ni–RE nanocrystalline alloys for hydrogen storage. Materials Science & Engineering A: Structural Materials: Properties, Microstructure and Processing, 2004, 375-377, 794-799.	2.6	139
9	Kinetic study of isothermal and continuous heating crystallization in GeSe2î—,GeTeî—,Sb2Te3 alloy glasses. Journal of Non-Crystalline Solids, 1983, 58, 209-217.	1.5	136
10	Improving the energy product of hard magnetic materials. Physical Review B, 2002, 65, .	1.1	112
11	Microstructural effects and large microhardness in cobalt processed by high pressure torsion consolidation of ball milled powders. Acta Materialia, 2003, 51, 6385-6393.	3.8	106
12	Size-Dependent Passivation Shell and Magnetic Properties in Antiferromagnetic/Ferrimagnetic Core/Shell MnO Nanoparticles. Journal of the American Chemical Society, 2010, 132, 9398-9407.	6.6	106
13	Room-temperature coercivity enhancement in mechanically alloyed antiferromagnetic-ferromagnetic powders. Applied Physics Letters, 1999, 75, 3177-3179.	1.5	105
14	Coercivity and squareness enhancement in ball-milled hard magnetic–antiferromagnetic composites. Applied Physics Letters, 2001, 79, 1142-1144.	1.5	103
15	Yielding and intrinsic plasticity of Ti–Zr–Ni–Cu–Be bulk metallic glass. International Journal of Plasticity, 2009, 25, 1540-1559.	4.1	103
16	Exploiting Length Scales of Exchange-Bias Systems to Fully Tailor Double-Shifted Hysteresis Loops. Advanced Materials, 2005, 17, 2978-2983.	11.1	102
17	Low phonon-energy glasses for efficient 1.3 î¼m optical fibre amplifiers. Electronics Letters, 1993, 29, 237.	0.5	101
18	Structural relaxation and rejuvenation in a metallic glass induced by shot-peening. Philosophical Magazine Letters, 2009, 89, 831-840.	0.5	98

2

#	Article	IF	CITATIONS
19	Enhanced mechanical properties and in vitro corrosion behavior of amorphous and devitrified Ti40Zr10Cu38Pd12 metallic glass. Journal of the Mechanical Behavior of Biomedical Materials, 2011, 4, 1709-1717.	1.5	97
20	Morphology, structure and magnetic properties of cobalt–nickel films obtained from acidic electrolytes containing glycine. Electrochimica Acta, 2011, 56, 1399-1408.	2.6	93
21	Nanocrystalline Electroplated Cu–Ni: Metallic Thin Films with Enhanced Mechanical Properties and Tunable Magnetic Behavior. Advanced Functional Materials, 2010, 20, 983-991.	7.8	92
22	Nanostructured β-phase Ti–31.0Fe–9.0Sn and sub-μm structured Ti–39.3Nb–13.3Zr–10.7Ta alloys fo biomedical applications: Microstructure benefits on the mechanical and corrosion performances. Materials Science and Engineering C, 2012, 32, 2418-2425.	or 3.8	90
23	Dynamic softening and indentation size effect in a Zr-based bulk glass-forming alloy. Scripta Materialia, 2007, 56, 605-608.	2.6	88
24	Enhanced mechanical properties due to structural changes induced by devitrification in Fe–Co–B–Si–Nb bulk metallic glass. Acta Materialia, 2010, 58, 6256-6266.	3.8	88
25	Magnetic Proximity Effect Features in Antiferromagnetic/Ferrimagnetic Core-Shell Nanoparticles. Physical Review Letters, 2009, 102, 247201.	2.9	85
26	Ni-, Pt- and (Ni/Pt)-doped TiO2 nanophotocatalysts: A smart approach for sustainable degradation of Rhodamine B dye. Applied Catalysis B: Environmental, 2016, 181, 270-278.	10.8	85
27	Microstructural and kinetic aspects of the transformations induced in a FeAl alloy by ball-milling and thermal treatments. Acta Materialia, 1998, 46, 3305-3316.	3.8	84
28	Electrodeposition of magnetic, superhydrophobic, non-stick, two-phase Cu–Ni foam films and their enhanced performance for hydrogen evolution reaction in alkaline water media. Nanoscale, 2014, 6, 12490-12499.	2.8	84
29	Influence of magnetization on the reordering of nanostructured ball-milled Fe-40 at. % Al powders. Physical Review B, 1998, 58, R11864-R11867.	1.1	82
30	Cold-consolidation of ball-milled Fe-based amorphous ribbons by high pressure torsion. Scripta Materialia, 2004, 50, 1221-1225.	2.6	81
31	Synthesis of compositionally graded nanocast NiO/NiCo2O4/Co3O4 mesoporous composites with tunable magnetic properties. Journal of Materials Chemistry, 2010, 20, 7021.	6.7	81
32	Hydrogen sorption performance of MgH2 doped with mesoporous nickel- and cobalt-based oxides. International Journal of Hydrogen Energy, 2011, 36, 5400-5410.	3.8	81
33	Mesoporous NiCo <sub>2</sub> O <sub>4</sub> Spinel: Influence of Calcination Temperature over Phase Purity and Thermal Stability. Crystal Growth and Design, 2009, 9, 4814-4821.	1.4	78
34	Exchange bias in ferromagnetic nanoparticles embedded in an antiferromagnetic matrix. International Journal of Nanotechnology, 2005, 2, 23.	0.1	77
35	Microstructural characterization of ultrafine-grained nickel. Physica Status Solidi A, 2003, 198, 263-271.	1.7	76
36	Strongly exchange coupled inverse ferrimagnetic soft/hard, MnxFe3â^'xO4/FexMn3â^'xO4, core/shell heterostructured nanoparticles. Nanoscale, 2012, 4, 5138.	2.8	76

#	Article	IF	CITATIONS
37	Origin of the large dispersion of magnetic properties in nanostructured oxides: Fe <sub>x</sub> O/Fe <sub>3</sub> O <sub>4</sub> nanoparticles as a case study. Nanoscale, 2015, 7, 3002-3015.	2.8	76
38	Improved mechanical performance and delayed corrosion phenomena in biodegradable Mg–Zn–Ca alloys through Pd-alloying. Journal of the Mechanical Behavior of Biomedical Materials, 2012, 6, 53-62.	1.5	72
39	Direct Magnetic Patterning due to the Generation of Ferromagnetism by Selective Ion Irradiation of Paramagnetic FeAl Alloys. Small, 2009, 5, 229-234.	5.2	71
40	Microstructural aspects of the hcp-fcc allotropic phase transformation induced in cobalt by ball milling. Philosophical Magazine, 2003, 83, 439-455.	0.7	69
41	Hydrogen desorption mechanism of 2NaBH4+MgH2 composite prepared by high-energy ball milling. Scripta Materialia, 2009, 60, 1129-1132.	2.6	69
42	Fracture surface morphology of compressed bulk metallic glass-matrix-composites and bulk metallic glass. Intermetallics, 2006, 14, 982-986.	1.8	66
43	Synthesis of amorphous Mg(BH4)2 from MgB2 and H2 at room temperature. Journal of Alloys and Compounds, 2010, 508, 212-215.	2.8	66
44	Grain Boundary Segregation and Interdiffusion Effects in Nickel–Copper Alloys: An Effective Means to Improve the Thermal Stability of Nanocrystalline Nickel. ACS Applied Materials & Interfaces, 2011, 3, 2265-2274.	4.0	63
45	Exchange bias effects in Fe nanoparticles embedded in an antiferromagnetic Cr2O3matrix. Nanotechnology, 2004, 15, S211-S214.	1.3	62
46	Volume expansion contribution to the magnetism of atomically disordered intermetallic alloys. Physical Review B, 2006, 74, .	1.1	59
47	Effect of relaxation and primary nanocrystallization on the mechanical properties of Cu60Zr22Ti18 bulk metallic glass. Intermetallics, 2005, 13, 1214-1219.	1.8	58
48	Effect of Transition Metal Fluorides on the Sorption Properties and Reversible Formation of Ca(BH <sub>4</sub> ) <sub>2</sub> . Journal of Physical Chemistry C, 2011, 115, 2497-2504.	1.5	58
49	Sorption properties of NaBH4/MH2 (M=Mg, Ti) powder systems. International Journal of Hydrogen Energy, 2010, 35, 5434-5441.	3.8	57
50	Role of stacking faults in the structural and magnetic properties of ball-milled cobalt. Physical Review B, 2003, 68, .	1.1	56
51	A comparison between fine-grained and nanocrystalline electrodeposited Cu–Ni films. Insights on mechanical and corrosion performance. Surface and Coatings Technology, 2011, 205, 5285-5293.	2.2	56
52	Two-, Three-, and Four-Component Magnetic Multilayer Onion Nanoparticles Based on Iron Oxides and Manganese Oxides. Journal of the American Chemical Society, 2011, 133, 16738-16741.	6.6	55
53	Correlation between stacking fault formation, allotropic phase transformations and magnetic properties of ball-milled cobalt. Materials Science & Engineering A: Structural Materials: Properties, Microstructure and Processing, 2004, 375-377, 869-873.	2.6	54
54	Structure and Thermodynamic Properties of the NaMgH <sub>3</sub> Perovskite: A Comprehensive Study. Chemistry of Materials, 2011, 23, 2317-2326.	3.2	54

#	Article	IF	CITATIONS
55	Pressure Effect on the 2NaH + MgB <sub>2</sub> Hydrogen Absorption Reaction. Journal of Physical Chemistry C, 2010, 114, 21816-21823.	1.5	53
56	Imprinting Vortices into Antiferromagnets. Physical Review Letters, 2006, 97, 067201.	2.9	51
57	Helical and Tubular Lipid Microstructures that are Electrolessâ€Coated with CoNiReP for Wireless Magnetic Manipulation. Small, 2012, 8, 1498-1502.	5.2	51
58	Microstructural inhomogeneities introduced in a Zr-based bulk metallic glass upon low-temperature annealing. Materials Science & Engineering A: Structural Materials: Properties, Microstructure and Processing, 2008, 491, 124-130.	2.6	50
59	Thermodynamic and Kinetic Investigations on Pure and Doped NaBH <sub>4</sub> â^'MgH <sub>2</sub> System. Journal of Physical Chemistry C, 2011, 115, 3151-3162.	1.5	50
60	Improvement to the Corrosion Resistance of Ti-Based Implants Using Hydrothermally Synthesized Nanostructured Anatase Coatings. Materials, 2014, 7, 180-194.	1.3	50
61	Can Na2[B12H12] be a decomposition product of NaBH4?. Physical Chemistry Chemical Physics, 2010, 12, 15093.	1.3	49
62	Kinetics of reordering of Ni3Al disordered by ball-milling. Acta Metallurgica Et Materialia, 1993, 41, 1065-1073.	1.9	48
63	Isothermal tuning of exchange bias using pulsed fields. Applied Physics Letters, 2003, 82, 3044-3046.	1.5	48
64	Plastic Deformation and Mechanical Softening of Pd40Cu30Ni10P20 Bulk Metallic Glass During Nanoindentation. Journal of Materials Research, 2005, 20, 2719-2725.	1.2	48
65	Mechanical properties of a two-phase amorphous Ni–Nb–Y alloy studied by nanoindentation. Scripta Materialia, 2007, 56, 85-88.	2.6	46
66	Experimental Evidence of Na2[B12H12] and Na Formation in the Desorption Pathway of the 2NaBH4+ MgH2System. Journal of Physical Chemistry C, 2011, 115, 16664-16671.	1.5	46
67	Direct evidence for an interdiffused intermediate layer in bi-magnetic core–shell nanoparticles. Nanoscale, 2014, 6, 11911-11920.	2.8	46
68	Facile <i>in Situ</i> Synthesis of BiOCl Nanoplates Stacked to Highly Porous TiO <sub>2</sub> : A Synergistic Combination for Environmental Remediation. ACS Applied Materials & Interfaces, 2014, 6, 13994-14000.	4.0	46
69	Effect of Nb addition on microstructure evolution and nanomechanical properties of a glass-forming Ti–Zr–Si alloy. Intermetallics, 2014, 46, 156-163.	1.8	45
70	Hardening and softening of FeAl during milling and annealing. Intermetallics, 2000, 8, 805-813.	1.8	44
71	Partial crystallization and corrosion resistance of amorphous Fe-Cr-M-B (M=Mo, Nb) alloys. Journal of Non-Crystalline Solids, 2010, 356, 2651-2657.	1.5	44
72	Bulk amorphous FeCrMoGaPCB: Preparation and magnetic properties. Journal of Magnetism and Magnetic Materials, 2005, 290-291, 1480-1482.	1.0	43

#	Article	IF	CITATIONS
73	Reversible post-synthesis tuning of the superparamagnetic blocking temperature of γ-Fe2O3nanoparticles by adsorption and desorption of Co(ii) ions. Journal of Materials Chemistry, 2007, 17, 322-328.	6.7	43
74	Enhanced Coercivity in Co-Rich Near-Stoichiometric CoxFe3-xO4+δ Nanoparticles Prepared in Large Batches. Chemistry of Materials, 2007, 19, 4957-4963.	3.2	43
75	Experimental Evidence of Ca[B12H12] Formation During Decomposition of a Ca(BH4)2 + MgH2 Based Reactive Hydride Composite. Journal of Physical Chemistry C, 2011, 115, 18010-18014.	1.5	43
76	Controlled Reduction of NiO Using Reactive Ball Milling under Hydrogen Atmosphere Leading to Niâ~'NiO Nanocomposites. Chemistry of Materials, 2004, 16, 5664-5669.	3.2	42
77	Enhanced mechanical properties in a Zr-based metallic glass caused by deformation-induced nanocrystallization. Scripta Materialia, 2010, 62, 13-16.	2.6	41
78	Voltageâ€Induced Coercivity Reduction in Nanoporous Alloy Films: A Boost toward Energyâ€Efficient Magnetic Actuation. Advanced Functional Materials, 2017, 27, 1701904.	7.8	41
79	Cold compaction of metal–ceramic (ferromagnetic–antiferromagnetic) composites using high pressure torsion. Journal of Alloys and Compounds, 2007, 434-435, 505-508.	2.8	40
80	Improved plasticity and corrosion behavior in Ti–Zr–Cu–Pd metallic glass with minor additions of Nb: An alloy composition intended for biomedical applications. Materials Science & Engineering A: Structural Materials: Properties, Microstructure and Processing, 2013, 559, 159-164.	2.6	40
81	Nanostructured Al88Ni4Sm8 alloys investigated by transmission electron and field-ion microscopies. Materials Science & Engineering A: Structural Materials: Properties, Microstructure and Processing, 2001, 304-306, 315-320.	2.6	39
82	Effects of the anion in glycine-containing electrolytes on the mechanical properties of electrodeposited Co–Ni films. Materials Chemistry and Physics, 2011, 130, 1380-1386.	2.0	39
83	Nanocasting of Mesoporous Inâ€TM (TM = Co, Fe, Mn) Oxides: Towards 3D Dilutedâ€Oxide Magnetic Semiconductor Architectures. Advanced Functional Materials, 2013, 23, 900-911.	7.8	38
84	Nanoindentation response of Cu–Ti based metallic glasses: Comparison between as-cast, relaxed and devitrified states. Journal of Non-Crystalline Solids, 2015, 425, 103-109.	1.5	38
85	Anelastic deformation of a Pd40Cu30Ni10P20 bulk metallic glass during nanoindentation. Applied Physics Letters, 2006, 88, 171911.	1.5	37
86	Glass forming ability of the Al–Ce–Ni system. Journal of Non-Crystalline Solids, 2008, 354, 4874-4877.	1.5	37
87	Activation of the reactive hydride composite 2NaBH4+MgH2. Scripta Materialia, 2011, 64, 1035-1038.	2.6	37
88	EEL spectroscopic tomography: Towards a new dimension in nanomaterials analysis. Ultramicroscopy, 2012, 122, 12-18.	0.8	37
89	Novel Fe–Mn–Si–Pd alloys: insights into mechanical, magnetic, corrosion resistance and biocompatibility performances. Journal of Materials Chemistry B, 2016, 4, 6402-6412.	2.9	37
90	Mechanical properties, corrosion performance and cell viability studies on newly developed porous Fe-Mn-Si-Pd alloys. Journal of Alloys and Compounds, 2017, 724, 1046-1056.	2.8	37

#	Article	IF	CITATIONS
91	Magnetic properties of ball milled Fe-40 Al at.% alloys. IEEE Transactions on Magnetics, 1998, 34, 1129-1131.	1.2	36
92	Optimisation of the ball-milling and heat treatment parameters for synthesis of amorphous and nanocrystalline Mg2Ni-based alloys. Journal of Alloys and Compounds, 2003, 349, 242-254.	2.8	36
93	Microstructural evolution during decomposition and crystallization of the Cu60Zr20Ti20 amorphous alloy. Journal of Materials Research, 2004, 19, 505-512.	1.2	36
94	Distinguishing the core from the shell in MnOx/MnOy and FeOx/MnOx core/shell nanoparticles through quantitative electron energy loss spectroscopy (EELS) analysis. Micron, 2012, 43, 30-36.	1.1	36
95	Resolving Material-Specific Structures within Fe <sub>3</sub> O <sub>4</sub>  î³-Mn <sub>2</sub> O <sub>3</sub> Core   Shell Nanoparticles Using Anomalous Small-Angle X-ray Scattering. ACS Nano, 2013, 7, 921-931.	7.3	36
96	Ca(BH <sub>4</sub> ) <sub>2</sub> + MgH <sub>2</sub> : Desorption Reaction and Role of Mg on Its Reversibility. Journal of Physical Chemistry C, 2013, 117, 3846-3852.	1.5	35
97	The influence of composition and low temperature annealing on hardness and ductility of rapidly solidified Al–Ni–Ce alloys. Scripta Materialia, 2002, 47, 31-37.	2.6	34
98	Crystallization of a Al–4Ni–6Ce glass and its influence on mechanical properties. Acta Materialia, 2003, 51, 1067-1077.	3.8	33
99	Direct Synthesis of Isolated L10 FePt Nanoparticles in a Robust TiO2 Matrix via a Combined Sol–Gel/Pyrolysis Route. Advanced Materials, 2006, 18, 466-470.	11.1	33
100	3D hierarchically porous Cu–BiOCl nanocomposite films: one-step electrochemical synthesis, structural characterization and nanomechanical and photoluminescent properties. Nanoscale, 2013, 5, 12542.	2.8	33
101	Evaluation of the Volume Fraction Crystallised during Devitrification of Al-Based Amorphous Alloys. Materials Science Forum, 2000, 343-346, 365-370.	0.3	32
102	Glass forming ability and crystallisation processes within the Al–Ni–Sm system. Journal of Non-Crystalline Solids, 2001, 289, 214-220.	1.5	31
103	Ultraporous Single Phase Iron Oxideâ^'Silica Nanostructured Aerogels from Ferrous Precursors. Langmuir, 2004, 20, 1425-1429.	1.6	31
104	Cold Consolidation of Metal–Ceramic Nanocomposite Powders with Large Ceramic Fractions. Advanced Functional Materials, 2008, 18, 3293-3298.	7.8	31
105	Effects of severe plastic deformation on the structure and thermo-mechanical properties of Zr55Cu30Al10Ni5 bulk metallic glass. Journal of Alloys and Compounds, 2010, 500, 61-67.	2.8	31
106	Mechanical and corrosion behaviour of as-cast and annealed Zr60Cu20Al10Fe5Ti5 bulk metallic glass. Intermetallics, 2012, 28, 149-155.	1.8	31
107	Room temperature magnetic hardening in mechanically milled ferromagnetic–antiferromagnetic composites. Journal of Magnetism and Magnetic Materials, 2000, 219, 53-57.	1.0	30
108	High-coercivity ultralight transparent magnets. Applied Physics Letters, 2003, 82, 4307-4309.	1.5	30

#	Article	IF	CITATIONS
109	Hydriding/dehydriding properties of nanocrystalline Mg87Ni3Al3M7 (M=Ti, Mn, Ce, La) alloys prepared by ball milling. Journal of Alloys and Compounds, 2005, 398, 139-144.	2.8	30
110	Periodic Arrays of Micrometer and Sub-micrometer Magnetic Structures Prepared by Nanoindentation of a Nonmagnetic Intermetallic Compound. Advanced Materials, 2006, 18, 1717-1720.	11.1	30
111	Novel Ti–Zr–Hf–Fe Nanostructured Alloy for Biomedical Applications. Materials, 2013, 6, 4930-4945.	1.3	30
112	Selective generation of local ferromagnetism in austenitic stainless steel using nanoindentation. Applied Physics Letters, 2006, 89, 032509.	1.5	28
113	Amorphization of soft magnetic alloys by the mechanical alloying technique. Materials Science & Engineering A: Structural Materials: Properties, Microstructure and Processing, 1991, 134, 1368-1371.	2.6	27
114	Nanocrystallization in Mg83Ni17â^'xYx (x=0, 7.5) amorphous alloys. Journal of Alloys and Compounds, 2002, 345, 123-129.	2.8	27
115	Structurally and mechanically tunable molybdenum oxide films and patterned submicrometer structures by electrodeposition. Electrochimica Acta, 2015, 173, 705-714.	2.6	27
116	Two-fold origin of the deformation-induced ferromagnetism in bulk Fe <sub>60</sub> Al <sub>40</sub> (at.%) alloys. New Journal of Physics, 2008, 10, 103030.	1.2	25
117	Unconventional elastic properties, deformation behavior and fracture characteristics of newly developed rare earth bulk metallic glasses. Intermetallics, 2009, 17, 1090-1097.	1.8	25
118	Chemical State, Distribution, and Role of Ti- and Nb-Based Additives on the Ca(BH <sub>4</sub> ) <sub>2</sub> System. Journal of Physical Chemistry C, 2013, 117, 4394-4403.	1.5	25
119	Improved fluoride glasses for 1.3 μ4m optical amplifiers. Journal of Non-Crystalline Solids, 1993, 161, 257-261.	1.5	24
120	Structural, mechanical and magnetic properties of nanostructured FeAl alloys during disordering and thermal recovery. Scripta Materialia, 1999, 11, 689-695.	0.5	24
121	Thermal characterization of Cu60ZrxTi40â^'x metallic glasses (x=15, 20, 22, 25, 30). Intermetallics, 2004, 12, 1063-1067.	1.8	24
122	On the biodegradability, mechanical behavior, and cytocompatibility of amorphous Mg <sub>72</sub> Zn <sub>23</sub> Ca <sub>5</sub> and crystalline Mg <sub>70</sub> Zn <sub>23</sub> Ca <sub>5</sub> Pd <sub>2</sub> alloys as temporary implant materials. Journal of Biomedical Materials Research - Part A, 2013, 101A, 502-517.	2.1	24
123	Crystallization behavior of some melt spun Nd–Fe–B alloys. Journal of Materials Research, 1990, 5, 1201-1206.	1.2	23
124	Evaluation of the anatase/rutile phase composition influence on the photocatalytic performances of mesoporous TiO2 powders. International Journal of Hydrogen Energy, 2015, 40, 14483-14491.	3.8	23
125	Designing new biocompatible glassâ€forming Ti <sub>75â€</sub> <i><sub>x</sub></i> Zr <sub>10</sub> Nb <i><sub>x</sub></i> Si <sub>15</sub> ( <i>x</i> = 0, 15) alloys: corrosion, passivity, and apatite formation. Journal of Biomedical Materials Research - Part B Applied Biomaterials. 2016. 104. 27-38.	1.6	23
126	Tailoring Staircase-like Hysteresis Loops in Electrodeposited Trisegmented Magnetic Nanowires: a Strategy toward Minimization of Interwire Interactions. ACS Applied Materials & 2016, 8, 4109-4117.	4.0	23

#	Article	IF	CITATIONS
127	Controlling magnetic vortices through exchange bias. Applied Physics Letters, 2006, 88, 042502.	1.5	22
128	Micelleâ€Assisted Electrodeposition of Mesoporous Fe–Pt Smooth Thin Films and their Electrocatalytic Activity towards the Hydrogen Evolution Reaction. ChemSusChem, 2018, 11, 367-375.	3.6	22
129	Stability and crystallization of Fe–Co–Nb–B amorphous alloys. Journal of Non-Crystalline Solids, 2004, 333, 320-326.	1.5	21
130	The effect of saccharine on the localized electrochemical deposition of Cu-rich Cu–Ni microcolumns. Electrochemistry Communications, 2011, 13, 973-976.	2.3	21
131	Hydrogen storage in 2NaBH4+MgH2 mixtures: Destabilization by additives and nanoconfinement. Journal of Alloys and Compounds, 2012, 536, S236-S240.	2.8	21
132	NaAlH4 confined in ordered mesoporous carbon. International Journal of Hydrogen Energy, 2013, 38, 8829-8837.	3.8	21
133	Magnetic investigations on the disordering of a ball milled Fe–40 Alat% alloy. Journal of Magnetism and Magnetic Materials, 1999, 203, 129-131.	1.0	20
134	Direct hydriding of Mg87Al7Ni3Mn3 by reactive mechanical milling in hydrogen atmosphere and influence of particle size on the dehydriding reaction. Journal of Alloys and Compounds, 2005, 388, 98-103.	2.8	20
135	Thermodynamic properties and absorption–desorption kinetics of Mg87Ni10Al3 alloy synthesised by reactive ball milling under H2 atmosphere. Journal of Alloys and Compounds, 2005, 404-406, 27-30.	2.8	20
136	The Influence of Deformationâ€Induced Martensitic Transformations on the Mechanical Properties of Nanocomposite Cuâ€Zrâ€(Al) Systems. Advanced Engineering Materials, 2011, 13, 57-63.	1.6	20
137	Electrodeposition of cobalt–yttrium hydroxide/oxide nanocomposite films from particle-free aqueous baths containing chloride salts. Electrochimica Acta, 2011, 56, 5142-5150.	2.6	20
138	Correlating material-specific layers and magnetic distributions within onion-like Fe3O4/MnO/γ-Mn2O3 core/shell nanoparticles. Journal of Applied Physics, 2013, 113, 17B531.	1.1	20
139	Role of aluminum chloride on the reversible hydrogen storageÂproperties of the Li–N–H system. International Journal of Hydrogen Energy, 2015, 40, 13506-13517.	3.8	20
140	Determination of T-T-T and T-HR-T curves from non-isothermal crystallization kinetic experiments. Thermochimica Acta, 1992, 203, 379-389.	1.2	19
141	Thermal stability, crystallization kinetics, and grain growth in an amorphous Al85Ce5Ni8Co2 alloy. Journal of Materials Research, 2002, 17, 2140-2146.	1.2	19
142	Synthesis and hydrogen sorption properties of nanocrystalline Mg1.9M0.1Ni (M=Ti, Zr, V) obtained by mechanical alloying. Journal of Alloys and Compounds, 2003, 356-357, 639-643.	2.8	19
143	Influence of the wheel speed on the thermal behaviour of Cu60Zr20Ti20 alloys. Materials Science & Engineering A: Structural Materials: Properties, Microstructure and Processing, 2004, 375-377, 776-780.	2.6	19
144	Microstructural characterization and hydrogenation study of extruded MgFe alloy. Journal of Alloys and Compounds, 2010, 504, S299-S301.	2.8	19

#	Article	IF	CITATIONS
145	2Mg–Fe alloys processed by hot-extrusion: Influence of processing temperature and the presence of MgO and MgH2 on hydrogenation sorption properties. Journal of Alloys and Compounds, 2011, 509, S460-S463.	2.8	19
146	Structural and magnetic characterization of batch-fabricated nickel encapsulated multi-walled carbon nanotubes. Nanotechnology, 2011, 22, 275713.	1.3	19
147	Mechanochemical synthesis of NaBH4 starting from NaH–MgB2 reactive hydride composite system. International Journal of Hydrogen Energy, 2013, 38, 2363-2369.	3.8	19
148	Structural and mechanical modifications induced on Cu47.5Zr47.5Al5 metallic glass by surface laser treatments. Applied Surface Science, 2014, 290, 188-193.	3.1	19
149	In vitro biocompatibility assessment of Ti40Cu38Zr10Pd12 bulk metallic glass. Journal of Materials Science: Materials in Medicine, 2014, 25, 163-172.	1.7	19
150	Evaporation-induced self-assembly synthesis of Ni-doped mesoporous SnO <sub>2</sub> thin films with tunable room temperature magnetic properties. Journal of Materials Chemistry C, 2017, 5, 5517-5527.	2.7	19
151	Effect of Surface Modifications of Ti40Zr10Cu38Pd12 Bulk Metallic Glass and Ti-6Al-4V Alloy on Human Osteoblasts In Vitro Biocompatibility. PLoS ONE, 2016, 11, e0156644.	1.1	19
152	Thermochemical parameters of the thermal dehydra-tion of trans[Crf(H2O)(1,3-diaminopropane)2][Ni(CN)4]. Thermochimica Acta, 1982, 56, 183-191.	1.2	18
153	A new temperature versus heating rate transformation (T-HR-T) diagram: Application to study the crystallization behaviour of Fe67.5Co15Nb1.5B16 metallic glass. Acta Metallurgica Et Materialia, 1992, 40, 37-42.	1.9	18
154	Outâ€ofâ€Plane Magnetic Patterning Based on Indentationâ€Induced Nanocrystallization of a Metallic Glass. Small, 2010, 6, 1543-1549.	5.2	18
155	Ammonia-free infiltration of NaBH4 into highly-ordered mesoporous silica and carbon matrices for hydrogen storage. Journal of Alloys and Compounds, 2013, 580, S309-S312.	2.8	18
156	Influence of the shot-peening intensity on the structure and near-surface mechanical properties of Ti40Zr10Cu38Pd12 bulk metallic glass. Applied Physics Letters, 2013, 103, 211907.	1.5	18
157	Mesoporous Titania Powders: The Role of Precursors, Ligand Addition and Calcination Rate on Their Morphology, Crystalline Structure and Photocatalytic Activity. Nanomaterials, 2014, 4, 583-598.	1.9	18
158	Sorption properties and reversibility of Ti(IV) and Nb(V)-fluoride doped-Ca(BH4)2–MgH2 system. Journal of Alloys and Compounds, 2015, 622, 989-994.	2.8	18
159	A facile co-precipitation synthesis of heterostructured ZrO2   ZnO nanoparticles as efficient photocatalysts for wastewater treatment. Journal of Materials Science, 2017, 52, 13779-13789.	1.7	18
160	Clustering analysis strategies for electron energy loss spectroscopy (EELS). Ultramicroscopy, 2018, 185, 42-48.	0.8	18
161	Evolution of amorphous and nanocrystalline phases in mechanically alloyed Mg1.9M0.1Ni (M=Ti,Zr,V). Journal of Alloys and Compounds, 2004, 381, 66-71.	2.8	17
162	Patterning of magnetic structures on austenitic stainless steel by local ion beam nitriding. Acta Materialia, 2008, 56, 4570-4576.	3.8	17

#	Article	IF	CITATIONS
163	Micelle-assisted electrodeposition of highly mesoporous Fe–Pt nodular films with soft magnetic and electrocatalytic properties. Nanoscale, 2017, 9, 18081-18093.	2.8	17
164	Relaxation processes below the glass transition in a GeSe2î—,GeTeî—,Sb2Te3 alloy. Journal of Non-Crystalline Solids, 1988, 104, 283-290.	1.5	16
165	Kinetics of Reordering in A Nanograined FeAl Alloy. Materials Science Forum, 1997, 235-238, 415-420.	0.3	16
166	Using exchange bias to extend the temperature range of square loop behavior in [Ptâ^•Co] multilayers with perpendicular anisotropy. Applied Physics Letters, 2005, 87, 242504.	1.5	16
167	Controlled generation of ferromagnetic martensite from paramagnetic austenite in AISI 316L austenitic stainless steel. Journal of Materials Research, 2009, 24, 565-573.	1.2	16
168	Electrodeposition of sizeable and compositionally tunable rhodium-iron nanoparticles and their activity toward hydrogen evolution reaction. Electrochimica Acta, 2016, 194, 263-275.	2.6	16
169	Nanocasting synthesis of mesoporous SnO <sub>2</sub> with a tunable ferromagnetic response through Ni loading. RSC Advances, 2016, 6, 104799-104807.	1.7	16
170	Electrochemically synthesized amorphous and crystalline nanowires: dissimilar nanomechanical behavior in comparison with homologous flat films. Nanoscale, 2016, 8, 1344-1351.	2.8	16
171	Tunable Magnetism in Nanoporous CuNi Alloys by Reversible Voltageâ€Driven Elementâ€5elective Redox Processes. Small, 2018, 14, e1704396.	5.2	16
172	Real time synchrotron studies on amorphous Al85Ce5Ni8Co2 and Al85Y5Ni8Co2 alloys. Journal of Alloys and Compounds, 2004, 368, 164-168.	2.8	15
173	Influence of the loading rate on the indentation response of Ti-based metallic glass. Journal of Materials Research, 2009, 24, 918-925.	1.2	15
174	Structural evolution upon decomposition of the LiAlH4+LiBH4 system. Journal of Alloys and Compounds, 2014, 615, S693-S697.	2.8	15
175	Measurements of structural relaxation in amorphous Fe40Ni40B20 by differential scanning calorimetry. Materials Science and Engineering, 1988, 97, 533-536.	0.1	14
176	Severe plastic deformation of a Ti-based nanocomposite alloy studied by nanoindentation. Intermetallics, 2007, 15, 1038-1045.	1.8	14
177	Drastic influence of minor Fe or Co additions on the glass forming ability, martensitic transformations and mechanical properties of shape memory Zr–Cu–Al bulk metallic glass composites. Science and Technology of Advanced Materials, 2014, 15, 035015.	2.8	14
178	Thermodynamic and thermokinetic characteristics of the glass transition in a GeSe2î—,GeTeî—,Sb2Te3 alloy. Journal of Non-Crystalline Solids, 1986, 86, 311-321.	1.5	13
179	Kinetics of Ordering in Ni <sub>3</sub> Al Based Alloys Disordered by Ball Milling. Materials Science Forum, 0, 88-90, 497-504.	0.3	13
180	Coercivity through controlled crystallization in melt-spun Ndî—,Feî—,B amorphous alloys. Journal of Alloys and Compounds, 1992, 182, 211-221.	2.8	13

#	Article	IF	CITATIONS
181	Calorimetric and X-Ray Measurements in Ultrafine-Grained Nickel. Materials Science Forum, 2003, 426-432, 4507-4512.	0.3	13
182	Mechanical behavior under nanoindentation of a new Ni-based glassy alloy produced by melt-spinning and copper mold casting. Journal of Non-Crystalline Solids, 2010, 356, 2251-2257.	1.5	13
183	Influence of the irradiation temperature on the surface structure and physical/chemical properties of Ar ion-irradiated bulk metallic glasses. Journal of Alloys and Compounds, 2014, 610, 118-125.	2.8	13
184	Thermochemical parameters of the thermal dehydration of trans-[CrF(H2O)(1,3-diaminopropane)2][M(CN)4] (M = Pd, Pt). Thermochimica Acta, 1983, 64, 237-246.	1.2	12
185	Glass-to-crystalline transformation in rapidly quenched Fe78B9Si13 ferromagnetic alloy. Journal of Non-Crystalline Solids, 1984, 69, 105-115.	1.5	12
186	Thermodynamic properties of nanocrystalline Ni3Al-based alloys prepared by mechanical attrition. Materials Science & Engineering A: Structural Materials: Properties, Microstructure and Processing, 1993, 168, 161-164.	2.6	12
187	Microstructure and hardness of a nanostructured Fe-40Al at% alloy. Scripta Materialia, 1999, 12, 801-806.	0.5	12
188	Influence of the milling conditions on the amorphization of Fe82Nb6B12 alloy. Journal of Non-Crystalline Solids, 2001, 287, 15-19.	1.5	12
189	Effect of the Milling Energy on the Milling-Induced hcp-fcc Cobalt Allotropic Transformations. Journal of Metastable and Nanocrystalline Materials, 2002, 12, 126-133.	0.1	12
190	Properties of FeNiB-based metallic glasses with primary BCC and FCC crystallisation products. Journal of Magnetism and Magnetic Materials, 2003, 254-255, 532-534.	1.0	12
191	Phase Separation and Crystallization in Cu-Zr Metallic Glasses. Materials Transactions, 2007, 48, 1639-1643.	0.4	12
192	Tailoring the magnetization reversal of elliptical dots using exchange bias (invited). Journal of Applied Physics, 2008, 103, 07C109.	1.1	12
193	Work-hardening mechanisms of the Ti <sub>60</sub> Cu <sub>14</sub> Ni <sub>12</sub> Sn <sub>4</sub> Nb <sub>10</sub> nanocomposite alloy. Journal of Materials Research, 2009, 24, 3146-3153.	1.2	12
194	Controlled 3D-coating of the pores of highly ordered mesoporous antiferromagnetic Co3O4 replicas with ferrimagnetic FexCo3â^'xO4 nanolayers. Nanoscale, 2013, 5, 5561.	2.8	12
195	Unravelling the Elusive Antiferromagnetic Order in Wurtzite and Zinc Blende CoO Polymorph Nanoparticles. Small, 2018, 14, e1703963.	5.2	12
196	The crystallization process of Ni78Si8B14 amorphous alloys. Materials Science and Engineering, 1988, 97, 333-336.	0.1	11
197	Enhanced microhardness in nanocomposite Ti60Cu14Ni12Sn4Ta10 processed by high pressure torsion. Intermetallics, 2006, 14, 871-875.	1.8	11
198	A Numerical Algorithm for Magnetohydrodynamics of Ablated Materials. Journal of Nanoscience and Nanotechnology, 2008, 8, 3674-3685.	0.9	11

#	Article	IF	CITATIONS
199	Ordered arrays of ferromagnetic, compositionally graded Cu1â^'xNix alloy nanopillars prepared by template-assisted electrodeposition. Journal of Materials Chemistry C, 2013, 1, 7215.	2.7	11
200	Enthalpy recovery in Se rich Geî—,Se glasses during isothermal annealing and continuous heating. Journal of Non-Crystalline Solids, 1991, 131-133, 479-482.	1.5	10
201	Preparation of Iron-Metalloid Amorphous Powders by Mechanical Alloying. Materials Science Forum, 1992, 88-90, 275-282.	0.3	10
202	Nanocrystallization of amorphous FeCuNbSiB based alloys. Scripta Materialia, 1995, 6, 461-464.	0.5	10
203	Correlation between the Microstructure and Enhanced Room Temperature Coercivity in Ball Milled Ferromagnetic - Antiferromagnetic Composites. Materials Science Forum, 2000, 343-346, 812-818.	0.3	10
204	Impact of magnetization easy-axis distributions on the ferromagnet-antiferromagnet exchange-coupling estimation. Physical Review B, 2008, 77, .	1.1	10
205	Tuning the microstructure and mechanical properties of Al-based amorphous/crystalline composites by addition of Pd. Intermetallics, 2010, 18, 2377-2384.	1.8	10
206	Anodic formation of self-organized Ti(Nb,Sn) oxide nanotube arrays with tuneable aspect ratio and size distribution. Electrochemistry Communications, 2013, 33, 84-87.	2.3	10
207	Temperature-heating rate transformation curves: a new tool for the study of crystallization. Journal Physics D: Applied Physics, 1992, 25, 803-807.	1.3	9
208	Preparation of Feî—,Ni based metal-metalloid amorphous powders by mechanical alloying. Materials Science & Engineering A: Structural Materials: Properties, Microstructure and Processing, 1994, 181-182, 1285-1290.	2.6	9
209	Crystallization mechanisms of a glassy alloy. Journal of Physics Condensed Matter, 1996, 8, 927-940.	0.7	9
210	Thermal stability and crystallization kinetics study of some Se-Te-Ge glassy alloys. Materials Science & Engineering A: Structural Materials: Properties, Microstructure and Processing, 1997, 226-228, 818-822.	2.6	9
211	Magnetic and Structural Properties of Mechanically Alloyed FexMn0.70?xAl0.30 (x = 0.40 and 0.45) Alloys. Physica Status Solidi A, 2002, 189, 811-816.	1.7	9
212	Influence of the heat treatment on the crystallization mechanisms of Al85Y5Ni8Co2 metallic glass. Journal of Non-Crystalline Solids, 2004, 343, 143-149.	1.5	9
213	Out-of-plane magnetic patterning on austenitic stainless steels using plasma nitriding. Applied Physics Letters, 2010, 96, 242509.	1.5	9
214	High-performance electrodeposited Co-rich CoNiReP permanent magnets. Electrochimica Acta, 2011, 56, 8979-8988.	2.6	9
215	Influence of the preparation method on the morphology of templated NiCo2O4 spinel. Journal of Nanoparticle Research, 2011, 13, 3671-3681.	0.8	9
216	Hydrogen storage properties of 2Mg–Fe mixtures processed by hot extrusion: Influence of the extrusion ratio. International Journal of Hydrogen Energy, 2012, 37, 15196-15203.	3.8	9

#	Article	IF	CITATIONS
217	Effects of shot peening on the nanoindentation response of Cu47.5Zr47.5Al5 metallic glass. Journal of Alloys and Compounds, 2014, 586, S36-S40.	2.8	9
218	Self-organized spatio-temporal micropatterning in ferromagnetic Co–In films. Journal of Materials Chemistry C, 2014, 2, 8259-8269.	2.7	9
219	Spontaneous formation of spiral-like patterns with distinct periodic physical properties by confined electrodeposition of Co-In disks. Scientific Reports, 2016, 6, 30398.	1.6	9
220	Kinetics of the thermal dehydration of trans-fluoroaquobis(ethylenediamine)chromium(III) tetracyanometallate(II) [metal(II) = Ni(II), Pd(II) and Pt(II)]. Thermochimica Acta, 1984, 80, 103-113.	1.2	8
221	Effect of the quenching conditions on the crystallization kinetics and morphology of Fe65Co18B16Si1. Materials Science & Engineering A: Structural Materials: Properties, Microstructure and Processing, 1991, 133, 807-810.	2.6	8
222	Correlation between microstructure and softmagnetic properties of FeCuNbSiB based alloys. Scripta Materialia, 1999, 12, 677-680.	0.5	8
223	Micro- and macroscopic magnetic study of the disordering (ball milling) and posterior reordering (annealing) of Fe-40 at.% Al. Journal of Non-Crystalline Solids, 2001, 287, 272-276.	1.5	8
224	Coercivity Enhancement in Ball-Milled and Heat-Treated Sr-Ferrite with Iron Sulphide. Journal of Metastable and Nanocrystalline Materials, 2003, 15-16, 599-606.	0.1	8
225	Thermal properties of Hf-based metallic glasses. Materials Science & Engineering A: Structural Materials: Properties, Microstructure and Processing, 2004, 375-377, 381-384.	2.6	8
226	Microstructural evolution during solid-state sintering of ball-milled nanocomposite WC–10 mass% Co powders. Nanotechnology, 2007, 18, 185609.	1.3	8
227	White-light photoluminescence and photoactivation in cadmium sulfide embedded in mesoporous silicon dioxide templates studied by confocal laser scanning microscopy. Journal of Colloid and Interface Science, 2013, 407, 47-59.	5.0	8
228	Tailoring the physical properties of electrodeposited CoNiReP alloys with large Re content by direct, pulse, and reverse pulse current techniques. Electrochimica Acta, 2013, 96, 43-50.	2.6	8
229	Thermodynamic aspects of glass-formation and crystallization in the GeSe2-S2Te3 system. Fluid Phase Equilibria, 1985, 20, 341-346.	1.4	7
230	Direct evidence of two different relaxation processes induced by heat treatment on Fe40Ni40B20glassy ribbons. Journal of Physics F: Metal Physics, 1988, 18, 2669-2681.	1.6	7
231	Thermoanalytical Characterization of a Nanograined Fe-40Al Alloy. Materials Science Forum, 1996, 225-227, 395-400.	0.3	7
232	Crystallization Mechanisms of some Se <sub>100–<i>x</i></sub> Te <sub><i>x</i></sub> Glassy Alloys. Journal of Materials Research, 1997, 12, 1069-1075.	1.2	7
233	Magnetic and X-Ray Diffraction Investigations of the Reordering of a Ball Milled Fe-40Al at% Alloy. Materials Science Forum, 1998, 269-272, 637-642.	0.3	7
234	Thermal stability and crystallization behavior of Fe77C5B4(AlGa)3(PSi)11 metallic glasses. Materials Science & Engineering A: Structural Materials: Properties, Microstructure and Processing, 2004, 375-377, 297-301.	2.6	7

#	Article	IF	CITATIONS
235	Influence of annealing on the microstructure and hardness of Ti67.79Fe28.36Sn3.85 nanocomposite rods. Scripta Materialia, 2006, 55, 1087-1090.	2.6	7
236	Comparative study of nanoindentation on melt-spun ribbon and bulk metallic glass with Ni60Nb37B3 composition. Journal of Materials Research, 2013, 28, 2740-2746.	1.2	7
237	Thermal studies on the anation and decomposition of trans-fluoroaquobis(ethylenediamine) and trans-fluoroaquoabis(propylenediamine) dithionate. Thermochimica Acta, 1981, 47, 271-276.	1.2	6
238	Thermodynamic and kinetic characterization of vitreous eutectic GeSe2î—,Sb2Te3 alloy. Thermochimica Acta, 1985, 85, 175-178.	1.2	6
239	Effect of magnetic interactions on the magnetic properties of ball-milled SmCo5+NiO powders. Journal of Magnetism and Magnetic Materials, 2002, 242-245, 1287-1289.	1.0	6
240	Deformation and fracture behavior of corrosion-resistant, potentially biocompatible, Ti40Zr10Cu38Pd12 bulk metallic glass. Journal of Alloys and Compounds, 2012, 536, S74-S77.	2.8	6
241	New binuclear copper( <scp>ii</scp> ) coordination polymer based on mixed pyrazolic and oxalate ligands: structural characterization and mechanical properties. RSC Advances, 2015, 5, 32369-32375.	1.7	6
242	Glass forming ability and crystallization kinetics of alloys in the GeSe2î—,GeTeî—,Sb2Te3 system. Journal of Non-Crystalline Solids, 1989, 111, 113-119.	1.5	5
243	Differential scanning calorimetry study of structural relaxation of Ge-doped Se85Te15 glasses. Materials Science and Engineering B: Solid-State Materials for Advanced Technology, 1994, 22, 181-190.	1.7	5
244	Optical fiber-drawing temperature of fluorogallate glasses. Journal of Materials Research, 1996, 11, 2633-2640.	1.2	5
245	Nanocrystallisation mechanisms in FeCuNbSiB-type alloys from comparative HREM, STM, TGM and calorimetric studies. Materials Science and Engineering B: Solid-State Materials for Advanced Technology, 1999, 63, 238-246.	1.7	5
246	Structural and Magnetic Characterization of High-Coercive Ball-Milled Hard Magnetic (SmCo <sub>5</sub> ) + Antiferromagnetic (NiO) Composites. Materials Science Forum, 2002, 386-388, 465-472.	0.3	5
247	Magnetic interaction effects on the hard magnetic properties of ball-milled SmCo5+NiO and SmCo5+CoO composites: A ΔM plot study. Journal of Applied Physics, 2003, 93, 8140-8142.	1.1	5
248	Tailoring deformation-induced effects in Co powders by milling them with α–Al <sub>2</sub> O <sub>3</sub> . Journal of Materials Research, 2007, 22, 2998-3005.	1.2	5
249	Evolution of the Mechanical Properties of Ti-Based Metallic Glass During Depth-Sensing Load–Unload Nanoindentation Cycles. Nanoscience and Nanotechnology Letters, 2010, 2, 298-302.	0.4	5
250	Hysteretic behaviour of melt-spun Nd13Fe79B8 after different crystallization treatments. Journal of Magnetism and Magnetic Materials, 1992, 104-107, 1141-1142.	1.0	4
251	Peculiarities accompanying the enthalpy recovery during structural relaxation of chalcogenic glasses. Journal of Non-Crystalline Solids, 1993, 163, 177-184.	1.5	4
252	Enthalpies of Formation ofL12Intermetallics Derived from Heats of Reordering. Physical Review Letters, 1997, 78, 4954-4957.	2.9	4

#	Article	IF	CITATIONS
253	Nanocrystallization Process in FeCuNbSiB Based Alloys. Materials Science Forum, 1999, 307, 95-100.	0.3	4
254	Magnetic investigations on the reordering of a ball milled Feî—,40Al at% alloy. Journal of Magnetism and Magnetic Materials, 1999, 196-197, 185-187.	1.0	4
255	Nanocrystallisation behaviour of Fe82Nb6B12 alloy. Materials Science & Engineering A: Structural Materials: Properties, Microstructure and Processing, 2001, 304-306, 296-299.	2.6	4
256	Magnetic Phase Diagram of the Fe <sub>x</sub> Mn <sub>0.60-x</sub> Al <sub>0.40</sub> (0.20 ≤ ≤0.60) Alloys Mechanically Alloyed for 48 Hours. Materials Science Forum, 2001, 360-362, 565-570.	0.3	4
257	Development of Hafnium-Based Bulk Metallic Glasses with large Supercooled Liquid Regions. Journal of Metastable and Nanocrystalline Materials, 2003, 15-16, 115-118.	0.1	4
258	Nanoscale phase separation in coated Ag nanoparticles. Nanoscale, 2011, 3, 4220.	2.8	4
259	Influence of the Si content on the microstructure and mechanical properties of Ti–Ni–Cu–Si–Sn nanocomposite alloys. Journal of Alloys and Compounds, 2012, 536, S186-S189.	2.8	4
260	Highly ordered mesoporous magnesium niobate high-Î⁰ dielectric ceramic: synthesis, structural/mechanical characterization and thermal stability. Journal of Materials Chemistry C, 2013, 1, 4948.	2.7	4
261	Nanomechanical behavior of 3D porous metal–ceramic nanocomposite Bi/Bi2O3 films. Materials Science & Engineering A: Structural Materials: Properties, Microstructure and Processing, 2015, 626, 150-158.	2.6	4
262	Room-temperature synthesis of three-dimensional porous ZnO@CuNi hybrid magnetic layers with photoluminescent and photocatalytic properties. Science and Technology of Advanced Materials, 2016, 17, 177-187.	2.8	4
263	Effect of Thermally-Induced Surface Oxidation on the Mechanical Properties and Corrosion Resistance of Zr60Cu25Al10Fe5 Bulk Metallic Glass. Science of Advanced Materials, 2014, 6, 27-36.	0.1	4
264	Magnetization versus heat treatment in rapidly solidified NdFeB alloys. IEEE Transactions on Magnetics, 1990, 26, 2613-2615.	1.2	3
265	Intergranular microstructure-coercive field relationship in Nd16Fe76B8 alloys. Journal of Magnetism and Magnetic Materials, 1993, 119, 289-293.	1.0	3
266	Thermal properties and crystallization kinetics of new fluoride glasses. Materials Science & Engineering A: Structural Materials: Properties, Microstructure and Processing, 1994, 179-180, 303-308.	2.6	3
267	New Gd-Al nanophase obtained by crystallization of Gd4Al3 metallic glass. Scripta Materialia, 1999, 12, 609-612.	0.5	3
268	Magnetic Hardening Induced by Exchange Coupling in Mechanically Milled Antiferromagnetic - Ferromagnetic Composites. Materials Research Society Symposia Proceedings, 1999, 581, 641.	0.1	3
269	Disordering of B2 Intermetallics by Ball Milling, with Particular Attention of FeAl. Materials Science Forum, 2001, 360-362, 195-202.	0.3	3
270	NaBX4-MgX2 Composites (X= D,H) Investigated by In situ Neutron Diffraction. Materials Research Society Symposia Proceedings, 2010, 1262, 1.	0.1	3

#	Article	IF	CITATIONS
271	Magnetic Measurements as a Sensitive Tool for Studying Dehydrogenation Processes in Hydrogen Storage Materials. Journal of Physical Chemistry C, 2010, 114, 16818-16822.	1.5	3
272	Sub-micron magnetic patterns and local variations of adhesion force induced in non-ferromagnetic amorphous steel by femtosecond pulsed laser irradiation. Applied Surface Science, 2016, 371, 399-406.	3.1	3
273	Caractérisation par A. T. D. de verres du système Se-Te-Ge0,5 Sb0,5. Revue De Physique Appliquée, 1977, 12 681-685.	' 0.4	3
274	Glass formation and crystallization in the GeSe2-GeTe-Sb2Te3 system. Thermochimica Acta, 1988, 133, 287-292.	1.2	2
275	Crystallization kinetic studies: A means to evaluate time-temperature-transformation curves. Application to metallic glasses. Journal of Thermal Analysis, 1991, 37, 1261-1268.	0.7	2
276	Influence of the Nature of Metalloid on the Morphology and Crystallization Kinetics of Fe-Co-B-Si Alloys. Key Engineering Materials, 1990, 40-41, 125-130.	0.4	2
277	Amorphous to Nanocrystalline Transformation in Fe <sub>77.5</sub> Cu <sub>1</sub> Nb <sub>3</sub> Si <sub>9.5Alloy. Materials Science Forum, 1996, 225-227, 347-352.</sub>	; <b>8</b> &dtsub8	& <b>g</b> t;9</sul
278	Influence of Co addition on the magnetic and thermal stability behavior of Fe77â^'Co Al2.14P8.4C5B4Ga0.86Si2.6 amorphous alloys. Journal of Magnetism and Magnetic Materials, 2004, 272-276, E1153-E1154.	1.0	2
279	Indentation plastic work and large compression plasticity in in situ nanocrystallized Zr62Cu18Ni10Al10 bulk metallic glass. Journal of Alloys and Compounds, 2011, 509, S87-S91.	2.8	2
280	2Mg-Fe Alloy Processed by Hot Extrusion: Influence of Particle Size and Extrusion Reduction Ratio on Hydrogenation Properties. Materials Science Forum, 0, 691, 3-9.	0.3	2
281	Unusual oxidation behavior of light metal hydride by tetrahydrofuran solvent molecules confined in ordered mesoporous carbon. Journal of Materials Research, 2014, 29, 55-63.	1.2	2
282	Cross-sectioning spatio-temporal Co-In electrodeposits: Disclosing a magnetically-patterned nanolaminated structure. Materials and Design, 2017, 114, 202-207.	3.3	2
283	H <sub>2</sub> sorption performance of NaBH <sub>4</sub> –MgH <sub>2</sub> composites prepared by mechanical activation. WIT Transactions on Ecology and the Environment, 2009, , .	0.0	2
284	Calorimetric Analyses of Mechanically Alloyed Ni <sub>3</sub> Al-Based Powders ( <l>Overview</l> ). Materials Transactions, JIM, 1995, 36, 341-350.	0.9	1
285	On the Role of Cu in the Nanocrystallization of Fe-Zr-Based Meltspun Amorphous Alloys. Materials Science Forum, 1995, 179-181, 569-574.	0.3	1
286	Evaluation of crystal nucleation and growth from crystallization kinetics data of new halide glasses. Journal of Non-Crystalline Solids, 1996, 205-207, 546-549.	1.5	1
287	Rapid Solidification and Mechanical Grinding of Cu-Zn Alloys. Materials Science Forum, 1997, 235-238, 571-576.	0.3	1
288	Correlation between thermal expansion and magnetic behavior in cold deformed Feî—,Al alloys. Journal of Magnetism and Magnetic Materials, 1999, 196-197, 240-242.	1.0	1

#	Article	IF	CITATIONS
289	Influence of annealing treatments on crystallization and mechanical properties of a Al–4Ni–6Ce glass. Materials Science & Engineering A: Structural Materials: Properties, Microstructure and Processing, 2004, 375-377, 965-968.	2.6	1
290	Thermal behaviour and corrosion characteristics of T78Si8B14 metallic glasses (T=Fe, Ni). Journal of Materials Science Letters, 1988, 7, 1336-1338.	0.5	0
291	Effect of the quenching conditions on the crystallization kinetics and morphology of Fe65Co18B16Si1. , 1991, , 807-810.		0
292	Thermal Evolution of Nanocrystalline Intermetallic Materials by DSC Measurements. Materials Science Forum, 1995, 179-181, 463-468.	0.3	0
293	Oxidation Influence on Crystallisation in Iron-Based Amorphous Alloys. Materials Science Forum, 2001, 360-362, 451-458.	0.3	0
294	Influence of the B Content on the Structural and Magnetic Properties of Fe <sub>60</sub> Mn <sub>10</sub> Al <sub>30-x</sub> B <sub>x</sub> Prepared by Mechanical Alloying. Materials Science Forum, 2002, 386-388, 497-502.	0.3	0
295	Crystallization of Al-Ni-Ce Glass and Implications for Control of Mechanical Properties during Powder Consolidation. Journal of Metastable and Nanocrystalline Materials, 2003, 15-16, 61-66.	0.1	0
296	Mechanical Characterization of Cu <sub>60</sub> Zr <sub>22</sub> Ti <sub>18</sub> Bulk Metallic Glasses. Journal of Metastable and Nanocrystalline Materials, 2005, 24-25, 669-672.	0.1	0
297	Crystallization of Amorphous Al <sub>85</sub> Ce <sub>5</sub> Ni <sub>10</sub> Ribbon. Materials Science Forum, 2008, 570, 126-131.	0.3	0
298	Progress Beyond the State-of-the-Art in the Field of Metallic Materials for Bioimplant Applications. , 2018, , 25-46.		0
299	The Crystallization Process of Ni78Si8B14 Amorphous Alloys. , 1988, , 333-336.		0